Can. J. Remote Sensing, Vol. 29, No. 2, pp. 141–153, 2003

Landsat TM and ETM+ thermal band calibration

J.A. Barsi, J.R. Schott, F.D. Palluconi, D.L. Helder, S.J. Hook, B.L. Markham, G. Chander, and E.M. O'Donnell

Abstract. Landsat-5 has been imaging the Earth since March 1984, and Landsat-7 was added to the series of Landsat instruments in April 1999. The Landsat Project Science Office and the Landsat-7 Image Assessment System have been monitoring the on-board calibration of Landsat-7 since launch. Additionally, two separate university teams have been evaluating the on-board thermal calibration of Landsat-7 through ground-based measurements since launch. Although not monitored as closely over its lifetime, a new effort is currently being made to validate the calibration of Landsat-5. Two university teams are beginning to collect ground truth under Landsat-5, along with using other vicarious calibration methods to go back into the archive to validate the history of the calibration of Landsat-5. This paper considers the calibration efforts for the thermal band, band 6, of both the Landsat-5 and Landsat-7 instruments. Though stable since launch, Landsat-7 had an initial calibration error of about 3 K, and changes were made to correct for this beginning 1 October 2000 for data processed with the National Landsat Archive Production System (NLAPS) and beginning 20 December 2000 for data processed with the Landsat Product Generation System (LPGS). Recent results from Landsat-5 vicarious calibration efforts show an offset of –0.7 K over the lifetime of the instrument. This suggests that historical calibration efforts may have been detecting errors in processing systems rather than changes in the instrument. A correction to the Landsat-5 processing has not yet been implemented but will be in the near future.

Résumé. Landsat-5 acquiert des images de la Terre depuis mars 1984 et Landsat-7 est venu s'ajouter à la série d'instruments Landsat en avril 1999. Le Bureau scientifique du projet Landsat (Landsat Project Science Office) et le système d'évaluation des images Landsat-7 (Landsat-7 image assessment system) étaient responsables du suivi de l'étalonnage à bord de Landsat-7 depuis son lancement. De plus, deux équipes universitaires se sont employées depuis son lancement à évaluer l'étalonnage thermique à bord de Landsat-7 par le biais de mesures au sol. Quoique Landsat-5 n'ait pas fait l'objet d'un suivi aussi soutenu durant sa durée de vie, un nouvel effort est en cours pour valider l'étalonnage de ce dernier. Deux équipes universitaires ont initié la collecte de données de réalité de terrain pour Landsat-5, tout en ayant recours à d'autres méthodes vicariantes d'étalonnage pour retourner dans l'archive afin de valider les données historiques de l'étalonnage de Landsat-5. Cet article focalise sur les efforts d'étalonnage relatifs à la bande 6, soit la bande thermique, des instruments Landsat-5 et Landsat-7. Quoique stable depuis son lancement, Landsat-7 a enregistré une erreur d'étalonnage de départ d'environ 3 K et des changements ont été apportés pour corriger cette situation à partir du 1 Octobre 2000, pour les données traitées avec le système NLAPS et, à partir du 20 Decembre 2000, pour les données traitées avec le système LPGS. Les résultats récents de ce travail d'étalonnage vicariant de Landsat-5 indiquent un décalage de –0,7 K au cours de la durée de vie de l'instrument laissant supposer que, dans le passé, les efforts d'étalonnage peuvent avoir détecté des erreurs dans les systèmes de traitement plutôt que des changements au niveau de l'instrument. Une correction de la procédure de traitement de Landsat-5 n'a pas encore été appliquée, mais elle le sera bientôt.
[Traduit par la Rédaction]

Introduction

Landsat satellites have been continuously acquiring Earth observation imagery since 1972. Seven Landsat satellites have been built, and six have been successfully launched and operated in orbit. Two remain operational: Landsat-5, launched in 1984; and Landsat-7, launched in 1999. The instruments on board these two satellites are very similar; the enhanced thematic mapper plus (ETM+) of Landsat-7 is a derivative of the thematic mapper (TM) on board Landsat-5.

Both satellites orbit at 705 km in a sun-synchronous orbit, with an equatorial crossing time of approximately 10:00 a.m. The repeat cycle is 16 days. Landsat-7 and Landsat-5 are 8 days offset from each other, so users benefit by having a Landsat

Received 1 March 2002. Accepted 13 August 2002.

J.A. Barsi.[1] Science Systems & Applications, Inc., NASA Goddard Space Flight Center, Code 923, Greenbelt, MD 20771, U.S.A.

J.R. Schott and E.M. O'Donnell. Rochester Institute of Technology, 74 Lomb Memorial Drive, Rochester, NY 14623, U.S.A.

F.D. Palluconi and S.J. Hook. NASA Jet Propulsion Laboratory, MS 183-501, 4800 Oak Grove Drive, Pasadena, CA 91109, U.S.A.

D.L. Helder. Electrical Engineering Department, South Dakota State University, Brookings, SD 57007, U.S.A.

B.L. Markham. NASA Goddard Space Flight Center, Code 923, Greenbelt, MD 20771, U.S.A.

G. Chander. Raytheon Information Technology and Scientific Services, EROS Data Center, U.S. Geological Survey, Sioux Falls, SD 57198, U.S.A.

[1]Corresponding author (e-mail: julia@ltpmail.gsfc.nasa.gov).

acquisition every 8 days. Both instruments are multispectral whisk-broom scanners with the same suite of bands (red, green, blue, near-infrared, two shortwave infrared, and a single longwave infrared). Enhancements to ETM+ from TM include increased spatial resolution of the thermal band (band 6), the addition of a panchromatic band, and the availability of each band of the ETM+ in two gain states (only one gain state is available for any given acquisition, except for the thermal band, which is always acquired in both gain states). **Table 1** compares selected features of the thermal band of both instruments. The increase of both the radiometric and spatial resolution has made the ETM+ thermal band more useful for studying human-scale factors.

Landsat-5

Landsat-5 was developed by the National Aeronautics and Space Administration (NASA) and initially operated by the National Oceanic and Atmospheric Administration (NOAA). In September 1985, operation of Landsat-5 was turned over to a private company, Earth Observation Satellite Company (EOSAT, now Space Imaging). In July 2001, the still-operational Landsat-5 and its entire image archives were turned back over to the U.S. government to be operated by the U.S. Geological Survey (USGS).

Over the lifetime of Landsat-5, there have been three U.S. processing systems to convert raw satellite digital numbers (DN) to calibrated radiance. The initial processing system for Landsat-5 was called the TM image processing system (TIPS), used by NOAA, and EOSAT adopted it when they took over. In October 1991, EOSAT updated their processing system to the enhanced image processing system (EIPS). The USGS archive, so far, has always been processed with the National Landsat Archive Production System (NLAPS)[2] (<http://edc.usgs.gov/glis/hyper/guide/landsat_tm.html>).

After an initial post-launch calibration verification sponsored by NASA, calibration efforts were either few and far between or mostly undocumented, particularly for the thermal band, during the period EOSAT was operating Landsat-5. At least one study indicated band 6 data products were out of calibration, but it is not known if a response was made to address this suggested miscalibration (Goetz et al., 1995). Now, with the increased availability of Landsat-5 data due to reduced cost, a recognition of the value of the archive for climate change study, and outside influence to validate the history of the archive for users, another NASA-sponsored calibration effort is underway for Landsat-5 data.

Teams from South Dakota State University (SDSU) and Rochester Institute of Technology (RIT) are being funded by NASA to collect new vicarious measurements for current Landsat-5 data along with using other techniques to calibrate historical data available in the archive.

Landsat-7

The Landsat-7 program is operated entirely by the government, a joint effort between the USGS and NASA. The program added two features to the Landsat-7 processing system to ensure the quality of calibrated data and less of a "black-box" approach to data products. The calibration parameter file (CPF) contains all information relevant to the radiometric and geometric calibration of ETM+ data. This file is issued with every data product and is used in processing it from raw data to calibrated data. CPFs are issued on a quarterly basis, for individual quarters, for all quarters since launch. Each scene is processed with a CPF issued for the specific quarter in which the scene was acquired. This allows for time-dependent calibration coefficients. Of importance here are the band 6 gains, offsets, and view coefficients, all calibration parameters

Table 1. Comparison of selected features of the thermal bands of TM and ETM+.

	Full-width half-maximum bandpass (μm)	Spatial resolution (m)	NEΔT (K at 280 K)	Radiometric scaling range ($W/m^2 \cdot sr \cdot \mu m$)[a]	Useful temperature range (K)
Landsat-5 TM	10.45–12.42	120	0.17–0.30	1.238–15.300	L1R 180–350; L1G 200–340
Landsat-7 ETM+	10.31–12.36	60	H 0.22; L 0.28	H 3.20–12.65; L 0.00–17.04	H 240–320; L 130–350

Note: Due to the build up of ice on the Landsat-5 dewar window, which effectively decreases the sensitivity of the detectors, the Landsat-5 noise equivalent change in temperature (NEΔT) is specified as a range and the useful temperature range is given for 16-bit radiance data (radiometrically corrected data (L1R), which varies with the sensitivity) and rescaled eight-bit data (radiometrically and geometrically corrected data (L1G), which is tied to the radiometric scaling range). The same measures are given separately for Landsat-7 high (H) and low (L) gain settings.

[a]Historically, Landsat-5 has used units of $mW/cm^2 \cdot sr \cdot \mu m$ and Landsat-7 uses units of $W/m^2 \cdot sr \cdot \mu m$. To be consistent in comparing Landsat-5 with Landsat-7, units of $W/m^2 \cdot sr \cdot \mu m$ are used, except for cases where values would be directly applied to the Landsat-5 images.

[2]The history of the U.S. ground-processing systems and their algorithms and processing parameters is poorly documented. In TIPS, at least initially, radiometric gains were calculated scan by scan using the internal calibrator, and the data were rescaled during processing to a standard dynamic range. Although used at the EOSAT, undocumented changes may have been made to TIPS. EIPS and NLAPS attempted to reconstruct the original TIPS processing algorithm for the thermal band; however, it has not been verified that the EIPS algorithm was implemented correctly.

contained in the CPF (available from <http://ltpwww.gsfc.nasa.gov/IAS/handbook/handbook_toc.html>).

The second improvement to the ETM+ processing system is the advent of the image analysis system (IAS). The IAS monitors the performance and calibration of ETM+ data on a daily basis by fully processing, through to geometric correction, a sampling of acquired scenes and storing individual scene results to a database (Storey et al., 1999). Through regular trending of the saved results, changes in instrument behavior can be monitored. The database currently contains approximately 3000 scenes worth of data. Additionally, the algorithms within the IAS are identical to those in the primary U.S. Landsat processing system, the Landsat Product Generation System (LPGS), so the IAS serves as a test bed for any algorithm modifications needed. Working closely with the IAS team at the USGS EROS Data Center (EDC) in Sioux Falls, South Dakota, the NASA Goddard Space Flight Center (GSFC) Landsat Project Science Office (LPSO) continually monitors the database trends and algorithm performance. Additional funding supports two thermal band vicarious calibration teams at the NASA Jet Propulsion Laboratory (JPL) and the RIT.

The teams from the IAS, LPSO, JPL, RIT, and SDSU and others involved in the calibration of the other bands meet on a semiannual basis to compile individual results. For Landsat-7, this includes making recommendations on updates to the radiometric gain calibration parameters in the CPF. For Landsat-5, the current emphasis is on determining the calibration history for the 18 year image archive and making recommendations on the appropriate corrections, if necessary. This paper focuses on the calibration of the thermal band (band 6) of both the TM and ETM+ instruments. This includes an attempt to retrieve the calibration history of Landsat-5, an opportunity for Landsat-5 and Landsat-7 cross-calibration, and recent vicarious calibration efforts for both instruments.

On-orbit calibration

The TM and ETM+ on-board thermal calibration systems consist of a single on-board cavity blackbody and a black, highly emissive shutter (**Figure 1**) (Markham et al., 1997). The blackbody sits off the optical axis at one of three temperatures. The shutter, which carries the calibration lamps across the optical axis for the visible calibration, has on it a toroidal mirror. As the shutter sweeps onto the optical axis, the mirror reflects the radiation from the blackbody onto the optics and through to the cooled focal plane. The non-mirror part of the shutter is coated with a high-emissivity paint and sits at the instrument ambient temperature. Outputs from thermistors located within TM and ETM+ monitoring temperatures of individual components are included in the downlinked data.

Landsat-5 equations

The Landsat-5 calibration equations make use of the blackbody and shutter and model contribution from the rest of the instrument. The optical components, baffles, and internal heaters contribute to the radiance reaching the detectors. This affect needs to be accounted for to provide imagery calibrated to ±5% (one sigma standard deviation). The model established for TM band 6 was based heavily on coefficients determined during pre-launch testing (Santa Barbara Research Center, 1984).

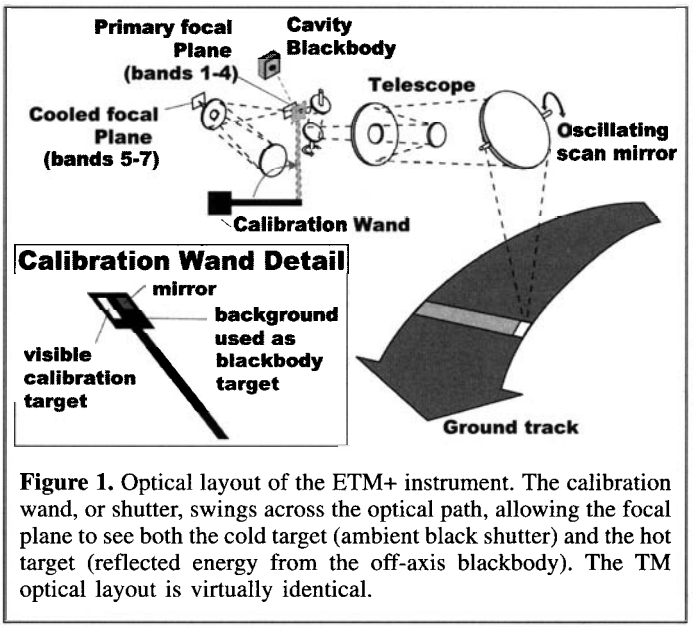

Figure 1. Optical layout of the ETM+ instrument. The calibration wand, or shutter, swings across the optical path, allowing the focal plane to see both the cold target (ambient black shutter) and the hot target (reflected energy from the off-axis blackbody). The TM optical layout is virtually identical.

The gain of the instrument is represented by the internal gain, G_{in}, and a factor that takes into account the fact that the calibration system does not pass through the entire optical system:

$$G_{in} = \frac{Q_{bb} - Q_{sh}}{L_{bb} - L_{sh}} \quad (1)$$

and

$$G_{ext} = aG_{in} \quad (2)$$

where Q_{bb} is the average digital number of the internal blackbody (calibration pulse); Q_{sh} is the average digital number of the shutter; L_{bb} is the spectral radiance of the blackbody as calculated from the blackbody temperature; L_{sh} is the spectral radiance of the shutter as calculated from the shutter temperature; and a is the pre-launch-determined gain ratio between the gain determined by the calibration system, G_{in}, and the gain of the full system, G_{ext}.

The offset term Q_0, or response of the instrument to a zero radiance signal, relies heavily on pre-launch coefficients:

$$Q_0 = Q_{sh} - G_{in}(bL_{sh} - c) \quad (3)$$

where b and c are pre-launch-determined coefficients that take into account the radiance contributed to the optical path by the instrument. Coefficients a, b, and c are given in **Table 2**.

Table 2. Calibration coefficients used in current Landsat-5 NLAPS processing (Goddard Space Flight Center, 1984).

Detector	a (unitless)	b (unitless)	c (mW/cm^2·sr·µm)
1	0.69	0.841	0.1702
2	0.65	0.841	0.2050
3	0.69	0.831	0.1646
4	0.64	0.829	0.2030

The gain and offset are used to convert the raw data to calibrated radiance:

$$L = \frac{Q - Q_0}{G_{ext}} \tag{4}$$

where Q is the digital number of an individual pixel; and L is the calculated radiance of that pixel.

Combining Equations (1), (2), (3), and (4) yields the overall calibration equation

$$L = \frac{L_{bb} - L_{sh}}{a(Q_{bb} - Q_{sh})}(Q - Q_{sh}) - \frac{1}{a}(bL_{sh} - c) \tag{5}$$

Users ordering calibrated image products, however, receive rescaled data that have also been geometrically corrected. No longer in units of radiance, the image has been rescaled to fit the entire range of an eight-bit system. Converting back to radiance requires knowledge of the original rescaling factors for radiance and DN:

$$L_{cal} = g_{rescale}Q_{cal} + b_{rescale} \tag{6}$$

where Q_{cal} is the digital number from the calibrated geometrically corrected imazge; L_{cal} is the calibrated radiance, the same as L in Equation (5) within the error of the rescaling process; and $g_{rescale}$ and $b_{rescale}$ are the rescaling factors. These factors are typically given in the header file. The current NLAPS header file (*.h1) lists these parameters as BAND#_RADIOMETRIC_GAINS/BIAS for $g_{rescale}$ and $b_{rescale}$. The current values are given in **Table 3**.

Although there has not been a systematic way to monitor the stability of the Landsat-5 gains and offsets, a study of the icing on the dewar window revealed the band 6 gain could be used as a prediction of the thickness of ice. Although this is not necessarily good for thermal band calibration, the compilation of these data shows how variable the external gain is over time (**Figure 2**). The band 6 gain was allowed to drop by 30% before the instrument would be outgassed.

Landsat-7 equations

In the case of ETM+ band 6, the gain is identical to the Landsat-5 gain (Equations (1) and (2)), although the coefficient is known as G_R. However, for the offset, rather than rely solely on temperature-independent coefficients to account for the contributions of the internal components, which change temperature as the instrument warms up, the effect of the components was empirically derived (Turtle, 1999). Five components were analytically determined to have a significant effect on the overall calibration: the scan-line corrector, the central baffle, the secondary mirror, the primary mirror, and the scan mirror. Their contribution is based on their temperature, their emissivity, and the extent to which they fill the field of view of the detector. Thus, the temperatures (by way of their radiances) of the components are included in the calculation of the offset term:

Table 3. Gain and bias to convert calibrated DN to calibrated radiance for a Landsat-5 NLAPS processed image.

Band	$g_{rescale}$ ((W/m^2·sr·µm)/counts)	$b_{rescale}$ (W/m^2·sr·µm)
TM 6	0.0551584	1.2378

$$Q_0 = Q_{sh} - G_R G_{in}\left[L_{sh} + \sum_{j=1}^{5} a_j(L_{sh} - L_j)\right] \tag{7}$$

where L_j is the spectral radiance from optical element j; and a_j is the view factor associated with optical element j. The a_j factors are stored in the CPF, and thus can be modified or added to without an overhaul of the processing system. Space was left in the CPF for the view factors of additional components, should they be deemed necessary upon calibration verification.

Combining Equations (1), (2), and (7), the final calibration equation for Landsat-7 is

$$L = \frac{L_{bb} - L_{sh}}{G_R(Q_{bb} - Q_{sh})}(Q - Q_{sh}) + L_{sh} + \sum_{j=1}^{5} a_j(L_{sh} - L) \tag{8}$$

Although the gain, G_{in}, and offset, DN_0, are calculated on a per-scan basis, they are not necessarily used on a per-scan basis in generating the calibrated image product. Within each processing system, parameters are set to select the source of the gain and offset terms. Each of these can come from either the individual scene itself, calculated as in Equations (2) and (7), or from the CPF. The gain and offset terms in the CPF are the average gain and offset of many scenes calculated from data in the IAS. Currently the LPGS processing system uses the per-scan calculated offset but the gain from the CPF. NLAPS, however, uses the CPF as the source of both gain and offset. Other processing systems may use other combinations of gains and biases.

The LPGS offers users the option to order data products in 16-bit radiance, known as L1R. This is the radiance calculated as in Equation (8). L1R products have been radiometrically corrected but not geometrically corrected. L1G products, the calibrated image products that include the geometric

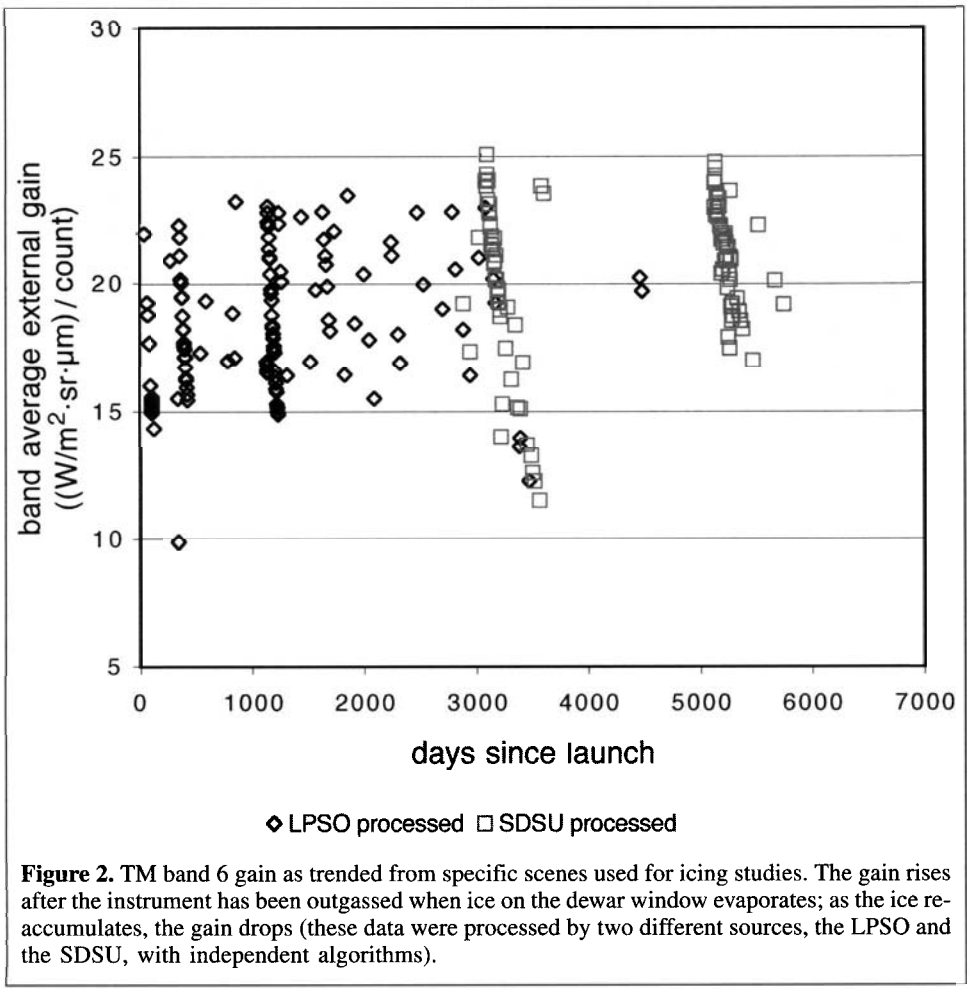

Figure 2. TM band 6 gain as trended from specific scenes used for icing studies. The gain rises after the instrument has been outgassed when ice on the dewar window evaporates; as the ice re-accumulates, the gain drops (these data were processed by two different sources, the LPSO and the SDSU, with independent algorithms).

correction, are rescaled to an eight-bit dynamic range. The equation to convert back to radiance is

$$L_{cal} = \frac{L_{max} - L_{min}}{Q_{max} - Q_{min}}(Q_{cal} - Q_{min}) + L_{min} \quad (9)$$

where L_{min}, L_{max}, Q_{min}, and Q_{max} are the rescaling factors.

Rescaling factors can be found in the image metadata (*.mtl) as the fields LMAX_BAND#, LMIN_BAND#, QCALMAX_BAND#, and QCALMIN_BAND# and are also given in **Table 4**.

Through the IAS, the Landsat-7 program has continually monitored the temperatures, gains, and biases calculated from the image data. The IAS has provided an invaluable tool in tracking system behavior. Problems have been detected early on due to regular monitoring of the trended data. For band 6, the instrument has been extremely stable. The per-scene external gain and biases are shown for the period between 28 June 1999 and 1 October 2000 in **Figure 3**. The gain varied by less than 0.5% (1 sigma standard deviation) and the bias by less than 1.5%. These results were extremely encouraging, suggesting a highly stable instrument. Although, the absolute radiometric calibration could not be inferred from this, by the fall of 2000, the vicarious calibration program had two successful collection seasons to evaluate the absolute calibration.

Vicarious calibration

Water is the primary target for thermal calibration because it is uniform in composition, has a high and known emissivity, and often exhibits low surface temperature variation (less than or equal to 1°C) over large areas. Land targets can provide a

Table 4. Rescaling factors to convert calibrated DN to calibrated radiance for a Landsat-7 LPGS or NLAPS processed image.

Band	L_{min} ($W/m^2 \cdot sr \cdot \mu m$)	L_{max} ($W/m^2 \cdot sr \cdot \mu m$)	Q_{min} counts		Q_{max} counts	
			NLAPS	LPGS	NLAPS	LPGS
6 (L)	0.0	17.04	0	1	255	255
6 (H)	3.2	12.65	0	1	255	255

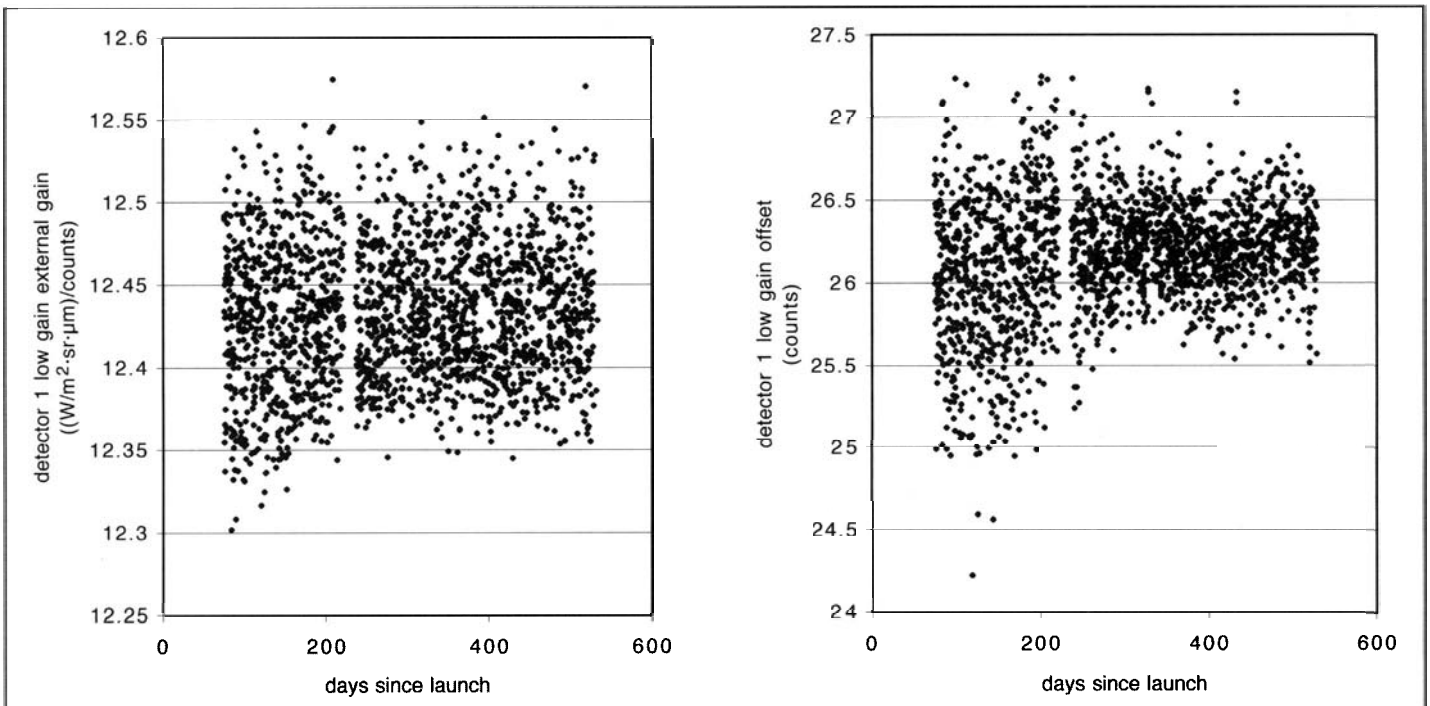

Figure 3. Trending results from the IAS database for Landsat-7 band 6 low gain. The data begin at the start of the operational period, 28 June 1999 (day 75 since launch), and go through 1 October 2000 (day 535 since launch). The gap at about day 225 is due to a broadcast error for which gain and biases cannot be compared with those for normal operations.

higher range of temperatures, although they are generally more difficult to characterize. The Landsat-5 and Landsat-7 vicarious calibration teams generally perform their work on water, but also use some very flat land targets to provide high-temperature verification.

Each calibration team has a slightly different method for propagating the ground, or in situ, temperature or radiance measurements to a top-of-atmosphere (TOA) radiance for direct comparison with the satellite-measured radiance. The general equation is

$$L_{TOA} = \tau L_{ground} + L_u \quad (10)$$

where L_{TOA} is the predicted TOA radiance for a target on the ground; L_{ground} is the surface-leaving radiance and includes the affects of both the emissivity of the target and the downwelling radiance of the atmosphere; τ is the transmission of the atmosphere; and L_u is the upwelling radiance of the atmosphere. In most cases, τ and L_u are derived using the local radiosonde as an input to MODTRAN (cf. Berk et al., 1989). See Schott et al. (2001) for more details on the individual techniques for propagating measured surface temperature or radiance to TOA radiance.

Landsat-5

Early on in the life of Landsat-5, the RIT performed the first verification of the thermal band calibration. Conclusions were that TM band 6 was calibrated to within ±0.9 K (Schott, 1988). Since this early look, no focused study of the calibration of TM band 6 has taken place. Recently, two teams have been investigating the calibration of the thermal band. The launch of Landsat-7 provided a unique opportunity for cross-calibration with Landsat-5; during the maneuvering of Landsat-7 to place it in the proper orbit, a 3 day period was scheduled where Landsat-5 and Landsat-7 were imaging coincident in location and nearly in time. The RIT investigated the calibration of Landsat-5 relative to Landsat-7, as well as taking ground truth under Landsat-5 at other opportunities. The JPL and SDSU have been using archived temperature data with the corresponding images of Lake Tahoe. One other study, the First International Satellite Land Surface Climatology Project (ISLSCP) Field Experiment (FIFE) in the late-1980s suggested that Landsat-5 band 6 was out of calibration by as much as 7°C. The LPSO has reexamined that study and found the Landsat-5 results no longer are applicable to currently processed data from that period.

RIT cross-calibration

During the on-orbit instrument verification period (OIVP), which lasted from launch on 15 April 1999 to 27 June 1999, Landsat-5 and Landsat-7 were scheduled to overlap in their acquisitions for a short period. With Landsat-5 operating at its standard 705 km, sun-synchronous orbit, Landsat-7 was positioned below Landsat-5 at 699 km for 4 days between 1 and 4 June 1999. Hundreds of nearly coincident scenes were acquired. One of these overlapping acquisitions was over Lake Michigan, during the occurrence of the thermal bar. This

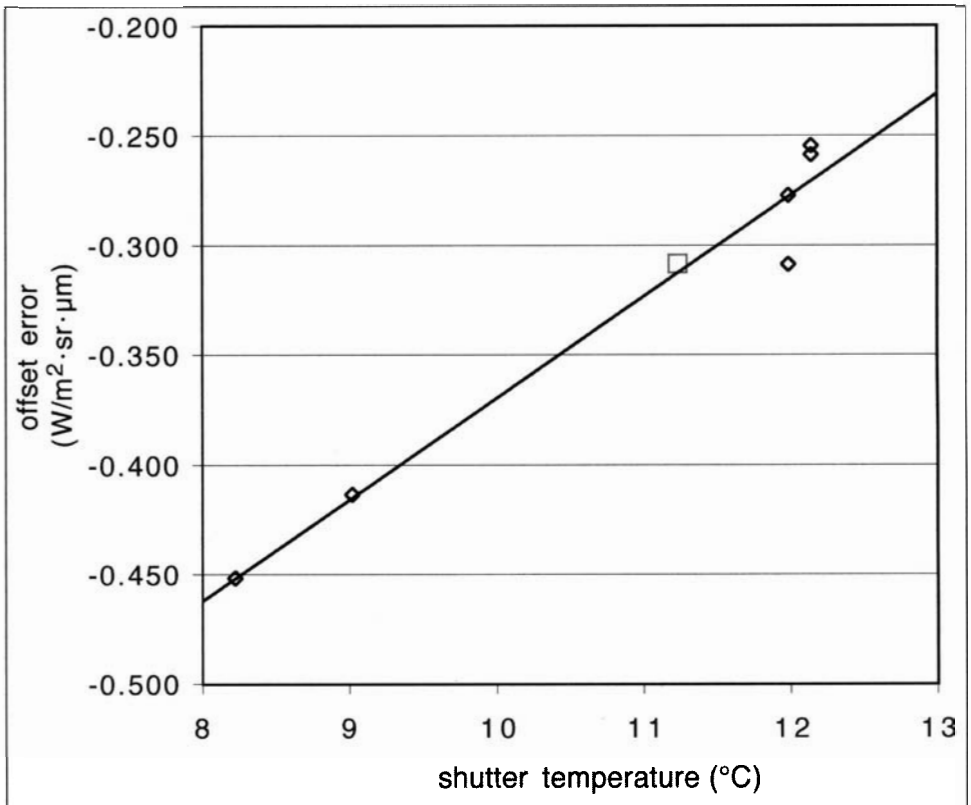

Figure 4. OIVP correlation between offset error and shutter temperature. The open diamonds are days for which ground truth was available, so the offset error was known; shutter temperatures of about 12°C are typical of normal operations. The open square is interpolated for 3 June 1999, the day on which the Lake Michigan data were acquired (the point is slightly off the trend line because it was calculated in radiance units and converted to temperature).

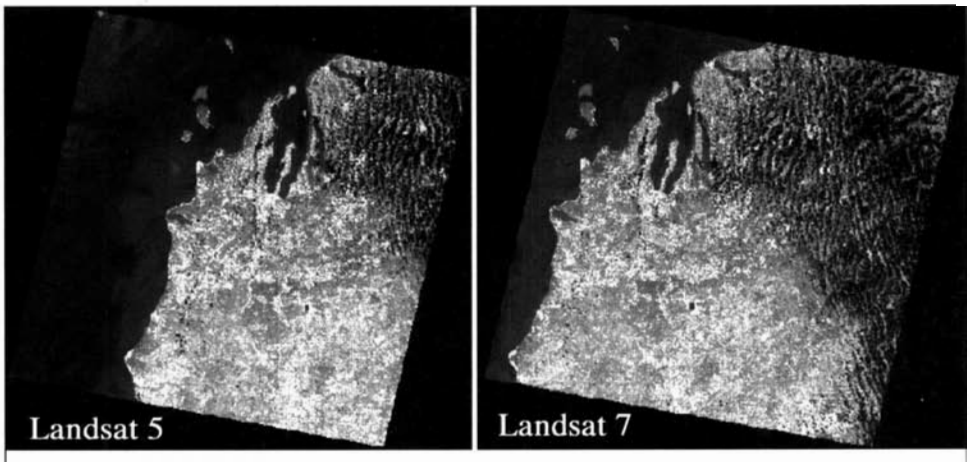

Figure 5. One of the pairs of Landsat-5 and Landsat-7 scenes used for the cross-calibration on 3 June 1999. Small regions throughout the scenes were compared directly. Note the visibility of the thermal bar, keeping warm water near shore and cold water in the center of the lake.

provided a well-characterized, stable target with a range of temperatures for thermal cross-calibration of the instruments.

The initial validation of the Landsat-7 calibration (see the next section) was performed before beginning this cross-calibration study so that Landsat-7 could be used as the reference instrument. Though the Landsat-7 calibration was found to be stable during normal operations when internal temperatures were constant, during OIVP, due to sporadic use, the internal temperatures were not stable, and this resulted in a temperature-dependent error in offset. Several vicarious campaigns were conducted during OIVP, so this variable offset could be determined and corrected for (**Figure 4**) based on a

high correlation between the error in offset and shutter temperature. The interpolated offset error was used to calibrate the Landsat-7 images, and TOA radiances could be compared with the Landsat-5 TOA radiances (**Figure 5**). The data are shown in (**Figure 6**).

RIT historical calibration

The goal of this historical calibration is to extract scenes from the archive for which some temperature within the scene is known, rather than having to have had ground truth for those scenes. The mid-lake regions of Lake Ontario during the winter and early spring are above 0°C, but below 4°C, as evidenced by the formation of the thermal bar later in the spring. Assuming large, uniform cold regions of lake water to be 1.5°C, the equivalent surface-leaving radiance was propagated to space and compared with the Landsat-5 imagery processed by the current NLAPS system. With error bars of nearly 2°C on the ground temperature estimation, this method serves as a loose verification of the historical data. This analysis only holds for the current NLAPS system; as shown later in the paper, some Landsat-5 products processed by EOSAT may not have been calibrated correctly. Data are shown in **Figure 6**.

JPL–SDSU

The JPL–SDSU group used the Lake Tahoe, California, automated validation site to help determine the absolute calibration of Landsat-5 band 6. The Lake Tahoe site was established to help validate data from instruments developed as part of the Earth-observing system, in particular, the advanced spaceborne thermal emission and reflectance radiometer (ASTER) and the moderate-resolution imaging spectroradiometer (MODIS). The site includes four rafts that are permanently anchored on the lake and continuously log the bulk water temperature, skin water temperature, and various meteorological variables (Hook et al.[3]). These data were used to perform an historical look at Landsat-5 calibration for multiple dates throughout 1999–2001. The results for 2000 are shown in **Figure 6**.

Also in this study, the SDSU verified the NLAPS processing algorithm (Chander et al., 2002). The SDSU is performing their analysis using 0R data, or raw image data. Using the TIPS calibration equations (Equations (1), (2), and (3)), the SDSU processed the raw data to radiance. Comparing several of these locally processed images to the same image processed to

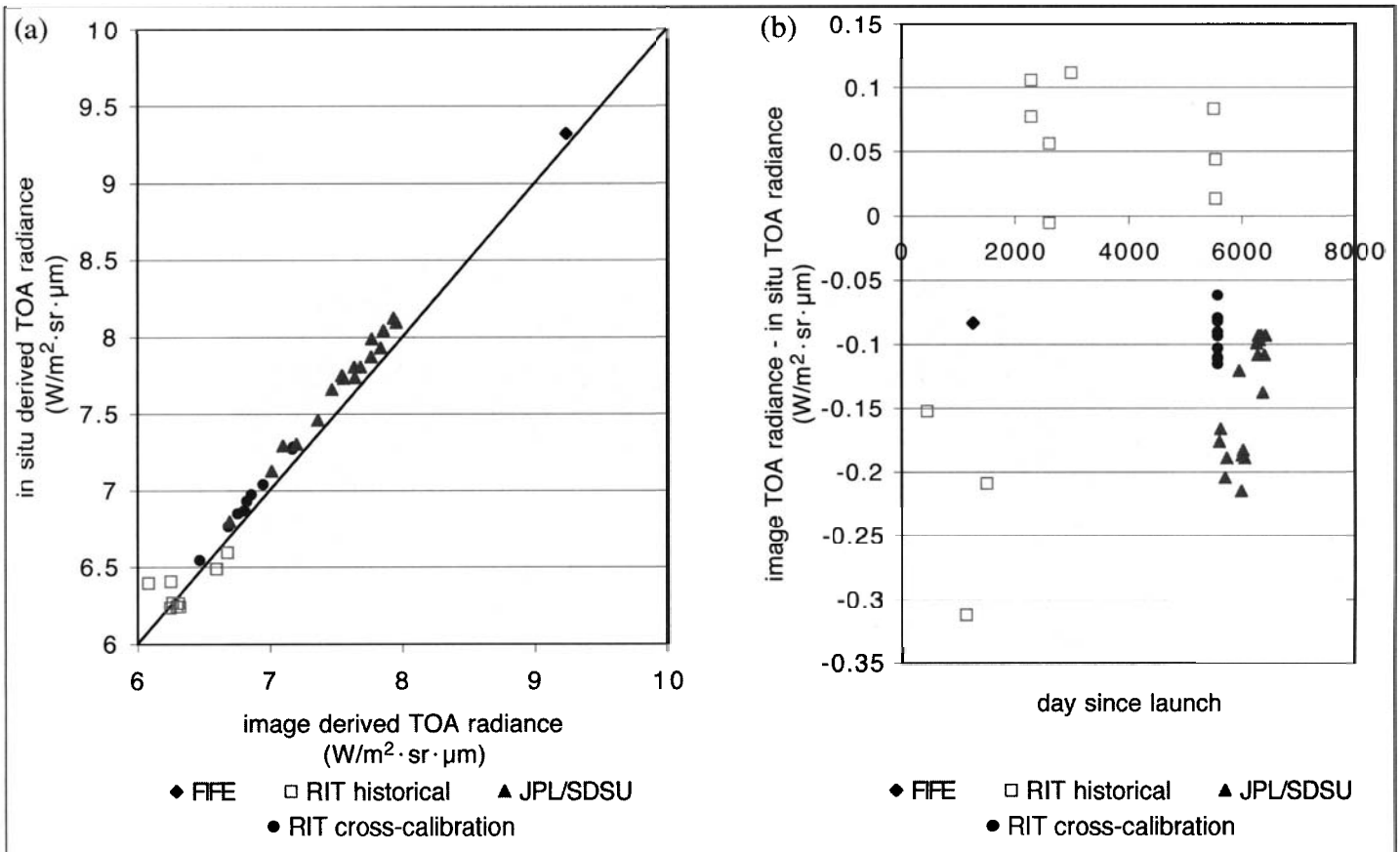

Figure 6. (*a*) Combined results of the Landsat-5 TM thermal band vicarious calibration efforts. (*b*) Difference between the image-predicted radiance and ground truth predicted radiance over time.

[3]S.J. Hook, A.J. Prata, R.E. Alley, A. Abtahi, R.C. Richards, S.G. Schladow, and S. Pálmarsson. Retrieval of lake bulk and skin temperatures using along track scanning radiometer (ATSR) data: a case study using Lake Tahoe, CA. *Journal of Atmospheric and Oceanic Technology*. In preparation.

radiance within NLAPS, the SDSU has verified that NLAPS is using the published TIPS algorithm correctly.

LPSO look at FIFE data

In a paper published in 1995 (Goetz et al., 1995), results from 1987 and 1989 reported TM band 6 to be predicting temperatures that were between 6° and 8°C too high. The original images were processed by the EOSAT TIPS system but could not be located. A subsampled subset of the original image of the collection site was contained on a CD-ROM archive from the FIFE campaign. For comparison, one of the same scenes was ordered from the current NLAPS processing system. The products yielded different results; the new NLAPS product appears to be calibrated based on the ground-truth results. Truth was provided by two near-surface instruments, an infrared thermometer (IRT) on the automated mesonet station (AMS) and an IRT mounted on a hand-held mast. **Table 5** shows the original results from the TIPS image as published in 1995 and the new analysis of the NLAPS product. There is also an issue with the model used to convert radiance to temperature; the coefficients in the FIFE paper do not match those in other published reports. This may have also accounted for 1°C of error.

These results suggest that the FIFE project had data where the radiometric calibration in the processing system was not implemented correctly. Since the original processing system no longer exists, there is no definite way to trace the problem to its source. Products generated in 1984 by this processing system appeared to be calibrated. This reexamination suggests that the current NLAPS products are calibrated to ±1°C, even for historical data products. The single data point is included in **Figure 6**.

Compiled results: RIT, JPL, SDSU, and FIFE

Although not rigorously monitored for nearly its entire lifetime, the compiled results indicate that Landsat-5 has not deteriorated as much as some papers have suggested. **Figure 6a** shows the combined results from the four vicarious calibration sources. Although most work has been done within the last 3 years, the RIT historical data serve an important function. Recall that this method is based on the assumption that the lake temperature is 1.5°C, whereas the actual temperature could range between 0° and 4°C. This leads to an error that is inherently a factor of two greater than the other methods. Considering this, the RIT historical data act as a bridge to the single FIFE point, to verify that nothing dramatic happened within the instrument over the 12 years between FIFE and Landsat-7. However, in the more recent data acquired between 1999 and 2001 and measured by the RIT cross-calibration and the JPL–SDSU, there is a distinct grouping of the data into two populations. The JPL–SDSU data are broken into groups versus time. No satisfactory explanation was made for the separation, either with the Landsat-5 instrument or with the instrumentation on the ground, although it seems clear that something happened. In light of this, for the final estimation of the error in offset, the JPL–SDSU data were divided into the two populations. The discontinuity occurs between September 2000 and April 2001, so the data were split between this point in **Figures 7** and **8**.

To reduce the data to a single prediction of error in offset, it was decided to treat all vicarious calibration methods equally, i.e., to remove the effect of the number of points. **Figure 7** shows the five data sets, namely FIFE, RIT cross-calibration, RIT historical, JPL–SDSU 1999–2000, and JPL–SDSU 2001, plotted, residuals versus image-derived TOA radiance.

The averaged compiled results from the five data sets suggest an offset error of 0.096 ± 0.026 $W/m^2 \cdot sr \cdot \mu m$, or –0.71 ± 0.20 K at 300 K, with Landsat-5 data being colder than the ground-truth data. There is no suggestion of any trend with time.

No action has been taken yet on this apparent calibration error, although the recommendation will be made to correct this within the NLAPS processing system by modifying the *c* calibration coefficient from Equation (5). Calibration updates and news about this upcoming change to the calibration system are available from <http://landsat7.usgs.gov/>.

Landsat-7

Two teams are responsible for verifying the calibration of Landsat-7, namely the RIT and the JPL. Both teams have been performing validation since launch and will continue their efforts for at least another 5 years.

RIT

The RIT team targets include Lake Erie and Lake Ontario and small bays and ponds adjoining the large lakes. The thermal bar, a spring phenomenon in large, temperate-zone lakes, provides an ideal target (Schott et al., 2001). Lasting for 4–6 weeks, the thermal bar prevents cold, winter-stratified water and warm, summer-stratified water from mixing uniformly in the lake, forming two large areas of uniform-temperature water separated by a distinct line. The separate warm and cold regions allow for a wider temperature range than a lake in normal conditions, where all surface water would equilibrate to the same temperature.

Table 5. Results from the original FIFE paper and from the newly processed scene.

	Radiance		Equivalent temperature (°C)			
	At-sensor	Atmospherically corrected	Exponential model	Planck model	IRT measured temperature (°C)	AMS measured temperature (°C)
FIFE archive image	9.911	10.995	38.452	39.350	32.066	30
NLAPS image	9.236	9.823	30.196	31.001	32.066	30

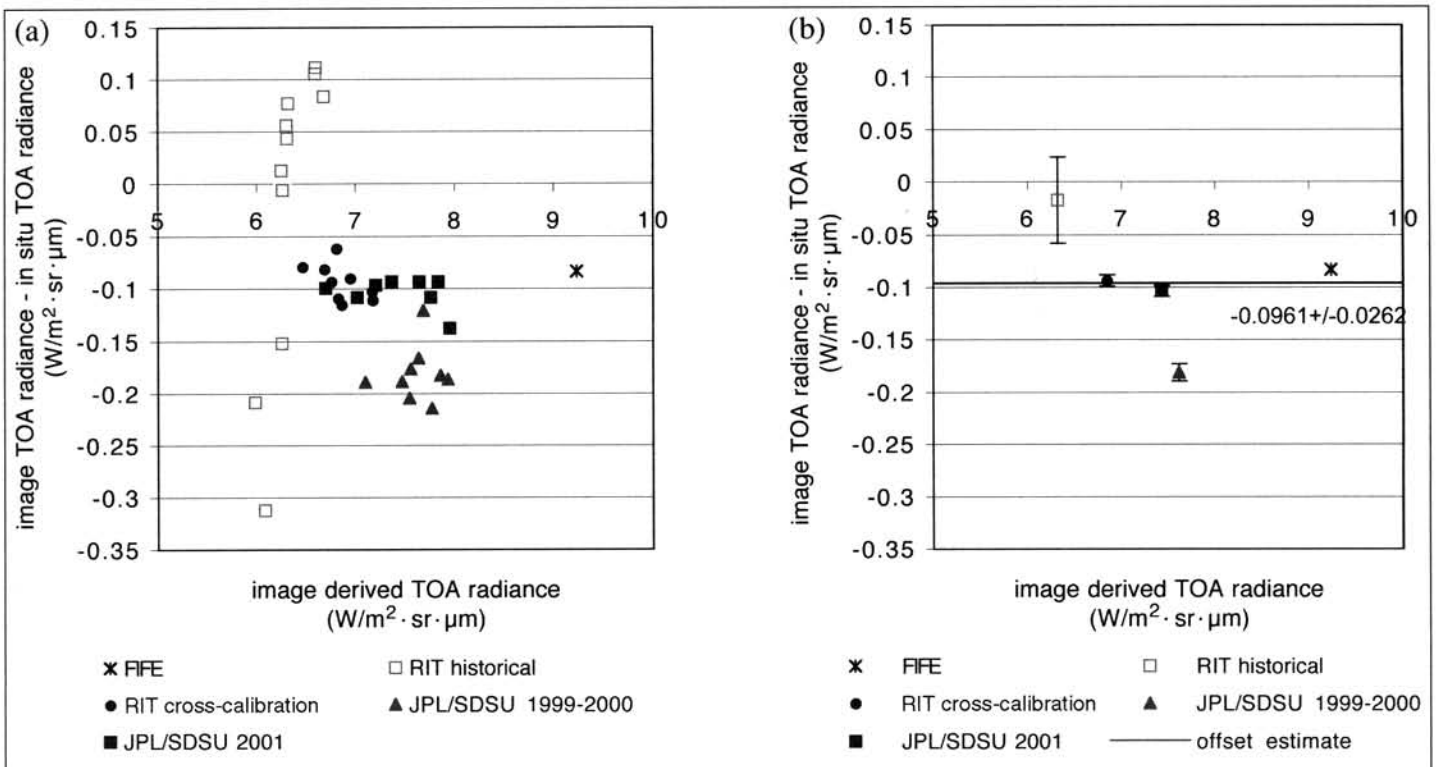

Figure 7. (*a*) Combined results of the Landsat-5 TM thermal band vicarious calibration residual error versus image-derived TOA radiance for the individual data points for each method. (*b*) The residuals of the methods are averaged and plotted against the average image-derived TOA radiance to estimate the error in offset. The average residual is the error in offset, shown as the shaded line (very close to the grid line at –0.1).

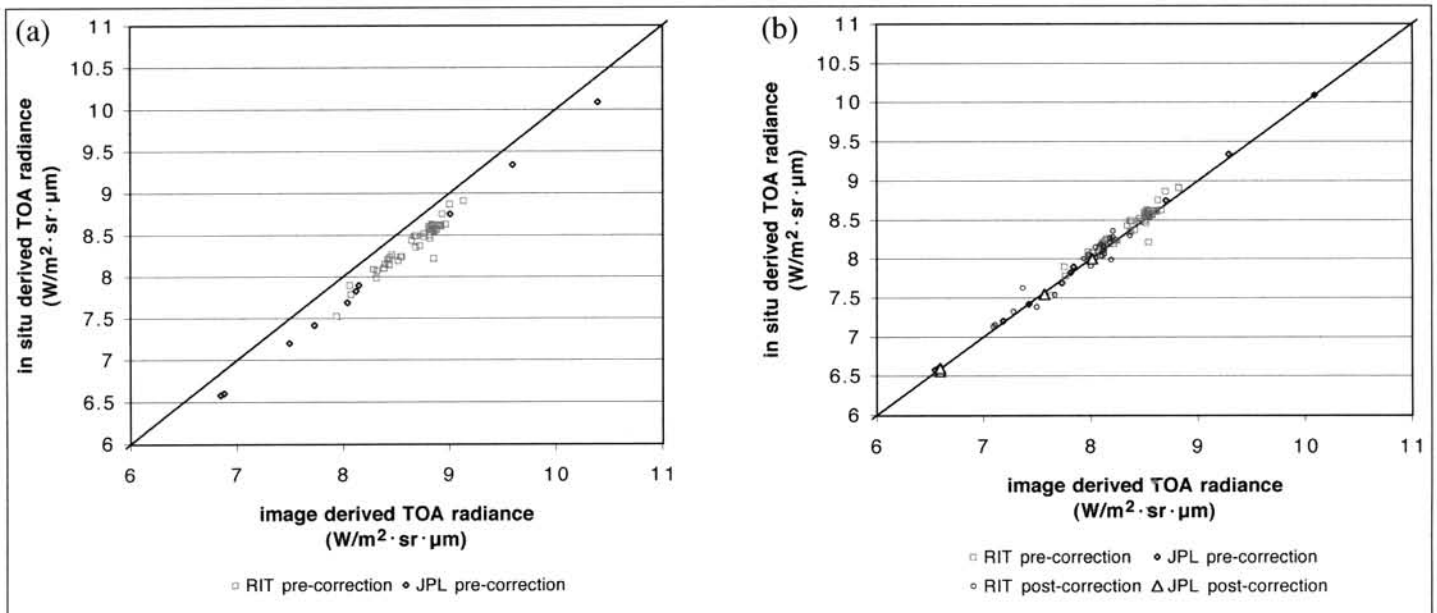

Figure 8. Compiled results of the ETM+ thermal band vicarious calibration teams. (*a*) The original calibration efforts revealed an error in offset. The correction was applied by introducing another calibration coefficient and modifying the equation. (*b*) The original calibration results processed with the updated system, along with data acquired after the correction was applied.

Using a collection of floating thermistors, a number of teams are deployed across the lake front. Canoe teams measure surface temperatures in small bays, ground teams measure surface temperatures in power plant discharge streams and off piers, and boat teams measure surface temperatures in the body of the lake, across the boundary of the thermal bar when present. Radiosonde data are routinely collected by the National Weather Service at the Buffalo, New York, airport (about 100 km) from the typical calibration site). With the assumption that the upper atmosphere is stable, the radiosonde

data are corrected for local surface conditions. These temperature and humidity radiosonde profiles are used as input into MODTRAN 3.5 to predict atmospheric transmission and upwelling radiance to propagate the lake water temperatures to TOA radiances. The satellite-measured radiances are compared with the in situ derived TOA radiances. Data are shown in **Figure 8a**.

JPL

The JPL calibration sites include Lake Tahoe, the Salton Sea, and assorted reservoirs within the large lake scenes. Five to nine buoys are dispersed over an area covering approximately 4 × 4 ETM+ pixels in area (240 × 240 m). These buoys measure and log the bulk water temperature at about 2–3 cm beneath the water surface. A radiometer simultaneously measures brightness temperature at one buoy location, which is used to determine the difference between the bulk water temperature and the water surface radiating temperature for all the buoy measurements. Several radiosondes are launched near the time of the expected ETM+ overflight to provide a profile estimate of air temperature and relative humidity. Sun photometer measurements are used to provide a measure of changes in atmospheric opacity and total column water vapor. Near-surface measurements observe wind velocity, air temperature, and relative humidity.

Using atmospheric profiles of water vapor and air temperature derived from the radiosondes, the spectral emissivity of water, and the spectral response of the radiometer, the water brightness temperature measurements are converted to surface kinetic temperature using a current version of the radiation transfer code MODTRAN 3.5. From this derivation, the bulk water to surface kinetic temperature difference is determined for the buoy nearest the radiometer, and this difference is applied across the array of buoys. This difference has always been between ±1°C, with almost all values being positive, i.e., the bulk water temperature is almost always higher than the derived water surface kinetic temperature. With the time of image acquisition known, the average derived water surface kinetic temperature is computed from the buoys in the array. In addition to deployable buoy arrays, the JPL operates four permanent rafts on Lake Tahoe, California, each equipped with bulk water temperature measuring sensors and radiometers (Hook et al.[3]). These are used to provide estimates of water kinetic temperature at the raft locations.

Although more difficult to characterize, land surface measurements are used to extend the range of comparison to higher radiance values than are accessible with water targets (i.e., above 32°C). The playa in Railroad Valley serves as the JPL land target. The procedure for land is similar to that used with water, substituting an array of two to five radiometers for the buoys to provide an estimate of the average surface brightness. Spectral emissivity of the surface is measured separately both in the field and with samples of the surface carried back to the laboratory for measurement. Data are shown in **Figure 8a**.

Compiled results

The compiled results through 1 October 2000 showed a significant bias: ETM+ was predicting higher than actual temperatures. Reducing the data, the bias was determined to be 0.31 W/m^2·sr·µm, or about 3 K at 300 K.

Applied correction

The bias of 0.31 W/m^2·sr·µm was accounted for by adjusting one of the pre-launch-determined view factors (Turtle, 1999). The pre-launch testing did not cover an adequate temperature range and specifically was not tested at the configuration of temperatures at which the satellite is currently operating. It was decided that these coefficients are the most likely source of the error. The five coefficients already in use were left as they were, but the shutter-view coefficient was added to the equation to compensate for the error in offset.

At the same time, the fundamental calibration was overhauled so that if, in the future, the internal instrument temperatures covered a wider range, the coefficients could be more easily re-derived on-orbit. The new equation includes the shutter-view factor in the offset term, modifying the shutter radiance and separating the shutter radiance from the other component radiances.

The gain term remains the same as that in the original version (Equations (1) and (2)), since there was no error in gain detected in the vicarious measurements. The offset term is now

$$Q_0 = Q_{sh} - G_R G_{in}\left(\frac{V_{sh}}{G_R} L_{sh} - \sum_{j=1}^{5} a_j L_j\right) \tag{11}$$

Equations (11) and (7) yield identical results if

$$\frac{V_{sh}}{G_R} = x + \sum a_j \tag{12}$$

where V_{sh} is the shutter-view factor, and $x = 1$; x is included in the equation to account for the error in radiance and was empirically derived using a number of scenes for which ground truth was available on a per-detector basis. For four of the scenes from the JPL and RIT campaigns, the derived factor agreed to within 0.5%. With the modification to the equation, V_{sh} no longer represents physical reality, but is a correction factor. The number that fills the V_{sh} spot in the CPF is

$$V_{sh} = G_R\left(x + \sum a_j\right) \tag{13}$$

The new factor and equation were tested for an average scene radiance change of 0.31 W/m^2·sr·µm on a collection of 17 miscellaneous images. For these 17 scenes, the average change in scene mean was 0.309 ± 0.003 W/m^2·sr·µm.

The offset term, Q_0, in the CPF was also updated to reflect the calibration error. The offset is in units of counts, so the new offset was changed by the change in counts equivalent to a change in radiance of 0.31 W/m^2·sr·µm.

Table 6. Calibration status of existing products from the U.S. systems where LPGS correction date is 20 December 2000 and NLAPS correction date is 1 October 2000.

System	Data acquired before correction date and processed before correction date	Data acquired before correction date and processed after correction date	Data acquired after correction date and processed after correction date
LPGS	Not calibrated, subtract 0.31 $W/m^2 \cdot sr \cdot \mu m$ from radiances	Calibrated	Calibrated
NLAPS	Not calibrated, subtract 0.31 $W/m^2 \cdot sr \cdot \mu m$ from radiances	Calibrated	Calibrated

Note: The acquisition date is the day the satellite acquired the image, and the processing date is the day the image was processed to either 1R or 1G by the processing system. These products are generated on demand, so the processing date will be close to the date on which the user received the data from the EDC.

It is hoped that eventually the instrument will be operated over a wide enough temperature range so the coefficients can be fully re-derived and V_{sh} would be replaced with a number that represents physical reality. However, over the nearly 3 years of operation, the internal instrument temperatures have not varied enough to enable this.

The new coefficients were initially released in the CPF release of 1 October 2000. However, the algorithm containing the new equation to calculate the offset was not implemented in the LPGS until 20 December 2000. Since NLAPS uses the values in the CPF, the correction was implemented in NLAPS with the release of the CPF on 1 October 2000.

Since the correction was implemented, another season of vicarious calibration was completed. The new collections from the RIT and the JPL both show good agreement with image-based radiances. The new data show no discernible offset within ±0.6 K uncertainty (one sigma standard deviation) (**Figure 8b**). Vicarious calibration will continue as the instrument ages, to continue to verify the absolute calibration of the Landsat-7 thermal band.

Summary and consequences for users

Landsat-7 band 6 data were found to have a 0.31 $W/m^2 \cdot sr \cdot \mu m$ error in bias since launch. This was causing Landsat-7 to predict surface temperatures about 3 K too high (at 300 K). This error was accounted for in the NLAPS processing system beginning 1 October 2000 and in the LPGS processing system beginning 20 December 2000. Since the correction was applied within the processing system, all data products ordered from these systems after the respective correction dates are calibrated, including images acquired both before and after the correction (**Table 6**). For data ordered previous to the implementation of the correction, the users can subtract 0.31 $W/m^2 \cdot sr \cdot \mu m$ from the radiance image product and consider these data calibrated. For data ordered from other processing systems, the user should check with the user services to see how the correction was implemented. Calibration notices are posted to several Web sites when calibration errors are found or changes to the parameters or processing system are made: the USGS Landsat-7 main page at <http://landsat7.usgs.gov/>, the IAS calibration notice page at <http://edcwww.cr.usgs.gov/l7dhf/ias_folder/cal_notes/>, and the Landsat-7 Science Data User's Handbook at <http://ltpwww.gsfc.nasa.gov/IAS/handbook/handbook_toc.html>.

Landsat-5 data have had mixed calibration results throughout its history, but it appears that some of the problem may have been caused by the processing system in use at the time. In at least one instance, data from the EOSAT TIPS system do not yield the same results as NLAPS. Data processed recently by NLAPS appear to have a slight offset error, –0.096 $W/m^2 \cdot sr \cdot \mu m$, with Landsat-5 data being about 0.7 K too cold. This error in offset has not been corrected for by the processing system as yet, but the recommendation to correct it will be made.

Landsat-7 data can be acquired from the USGS through the LPGS processing system (available from <http://edcimswww.cr.usgs.gov/pub/imswelcome/plain.html>) or through the NLAPS processing system (available from <http://earthexplorer.usgs.gov>). Landsat-5 data are only available through the NLAPS system (available from <http://earthexplorer.usgs.gov>).

References

Berk, A., Bernstein, L.S., and Robertson, D.C. 1989. *MODTRAN: a moderate resolution model for LOWTRAN 7.* Report GL-TE-89 0122, Geophysics Laboratory, Hanscom Airforce Base, Mass.

Chander, G., Helder, D., and Boncyk, W. 2002. Landsat-4/5 band 6 relative radiometry. *IEEE Transactions on Geoscience and Remote Sensing*, Vol. 40, No. 1, pp. 206–210.

Goetz, S.J., Halthore, R.N., Hall, F.G., and Markham, B.L. 1995. Surface temperature retrieval in a temperate grassland with multiresolution sensors. *Journal of Geophysical Research*, Vol. 100, No. D12, pp. 25 397 – 23 410.

Goddard Space Flight Center. 1984. *Landsat to ground station interface description: Appendix G.* Report 435-D-400, NASA Goddard Space Flight Center, Greenbelt, Md.

Markham, B.L., Boncyk, W.C., Helder, D.L., and Barker, J.L. 1997. Landsat-7 enhanced thematic mapper plus radiometric calibration. *Canadian Journal of Remote Sensing*, Vol. 23, No. 4, pp. 318–332.

Santa Barbara Research Center. 1984. *Thematic mapper calibration report flight model – Landsat-5 (contract NAS5-24200).* Santa Barbara Research Center, Santa Barbara, Calif.

Schott, J.R. 1988. Thematic mapper, band 6, radiometric calibration and assessment. *Proceedings of SPIE*, Vol. 924, pp. 72–88.

Schott, J.R., Barsi, J.A., Nordgren, B.L., Raqueño, N.G., and de Alwis, D. 2001. Calibration of Landsat thermal data and application to water resource studies. *Remote Sensing of Environment*, Vol. 78, pp. 108–117.

Storey, J., Morfitt, R., and Thorson, P. 1999. Image processing on the Landsat 7 image assessment system. In *Proceedings of the 1999 ASPRS Annual Conference, From Image to Information*, 17–21 May 1999, Portland, Oreg. CD-ROM. American Society for Photogrammetry and Remote Sensing, Bethesda, Md.

Turtle, R.R. 1999. ETM+ band 6 calibration report (PL2807E-T06298). Santa Barbara Research Center, Santa Barbara, Calif.